Cloud-Native Deployment of a Sinkhole Susceptibility Mapping Platform Using Google Earth Engine and Colab in Urbanised Karst Terrain

Tan Y.E. [1*] and Roslan S.N.A. [2]

[1]Master Student, Department of Civil Engineering, Faculty of Engineering, Universiti Putra Malaysia (UPM), Selangor, Malaysia

[2]Senior Lecturer, Department of Civil Engineering, Faculty of Engineering, Universiti Putra Malaysia (UPM), Selangor, Malaysia

*tanyaneng@gmail.com

***Abstract*:** *Sinkholes are increasingly recognised as critical geohazards in rapidly urbanising karst regions, where the dissolution of subsurface limestone or similar soluble rocks is accelerated by anthropogenic stressors such as leaking underground pipelines, groundwater extraction, and urban infrastructure loading. These processes can lead to sudden ground collapse, posing risks to public safety, property, and essential services. Despite their growing frequency, public access to sinkhole risk information remains limited, particularly in developing urban contexts like Kuala Lumpur, Malaysia, where fragmented datasets, restricted geotechnical records, and a lack of open-source modelling tools have hindered proactive hazard communication. This study presents a cloud-native platform for sinkhole susceptibility mapping that integrates multi-source geospatial data with deep learning and delivers results via an interactive web application, offering both technical scalability and public usability. The proposed workflow leverages Google Earth Engine (GEE) for geospatial data processing and Google Colab for model training, enabling a seamless end-to-end pipeline without reliance on desktop GIS tools. A one-dimensional Convolutional Neural Network (1D CNN) was selected due to its computational efficiency, strong generalisation performance, and suitability for this study's context in classifying sinkhole susceptibility based on 14 spatial control factors spanning geological, topographic, hydrological, and anthropogenic domains. The trained model outputs a continuous susceptibility surface, facilitating nuanced risk interpretation. Performance evaluation yielded a high AUC-ROC (0.97), confirming strong discriminatory power even with a limited training sample. The resulting susceptibility map is deployed via a public-facing GEE web application that includes toggleable data layers and interactive query functions designed for planners, engineers, and the general public. Unlike earlier study focused on model comparison, this work prioritises the deployment architecture and operational scalability of a fully cloud-native geospatial workflow. The platform supports scalable updates and future integration with real-time data sources. Overall, this study demonstrates the practical viability of cloud-native geospatial modelling for hazard assessment and public communication in data-limited urban contexts. It also provides a reproducible, user-friendly template for other rapidly developing cities facing similar challenges in managing subsurface risks associated with karst development.*

Keywords: Google Earth Engine, Karst, Sinkhole susceptibility, Convolutional Neural Network

Introduction

Urban sinkholes are increasingly recognised as critical geohazards, particularly in rapidly urbanising regions underlain by karst terrain (Ha, 2024). These hazards are typically associated with the dissolution of soluble rocks such as limestone, gypsum, or dolomite, which can lead to sudden surface collapse when compounded by anthropogenic stressors including construction, groundwater withdrawal, and underground utility failure (Ford & Williams, 2007; Waltham et al., 2005; Shi et al., 2021; Li et al., 2022; Ha, 2024). Both natural and human-induced processes contribute to subsurface instability and differential surface loading, resulting in severe environmental and socio-economic impacts such as ground collapse, infrastructure damage, service disruption, and, in extreme cases, loss of life (Gutiérrez et al., 2014; Yumba et al., 2024).

While sinkholes are a global concern, their impacts are particularly severe in rapidly transforming cities developed atop karst formations. This includes parts of Southeast Asia, the Middle East, southern Europe, and regions of North America and China (Zhou et al., 2016; Jia et al., 2021; Damayanti et al., 2021; Fartihul Ilmy et al., 2021; Park et al., 2022; Bianchini et al., 2022; Li et al., 2024; Mohammadi-Ahmadmahmoudi et al., 2025; García-Cruzado et al., 2025). In tropical Southeast Asia, where high rainfall and deep weathering intensify karst processes, urban centres like Kuala Lumpur face heightened risks. The Malaysian capital is underlain by the deeply karstified Kuala Lumpur Limestone Formation, which has been extensively overlain by engineered fill, infrastructure, and remnants of past tin mining activities (Tan, 2006; Rosdi et al., 2017; Banks et al., 2020).

Despite the rising frequency of sinkhole incidents in urban areas, public access to susceptibility information remains limited. In Malaysia, hazard communication for other geohazards, such as floods and landslides has benefited from web-based platforms like Public Infobanjir by Department of Irrigation and Drainage Malaysia and MyBahaya Platform by Universiti Kebangsaan Malaysia researchers. However, sinkhole mapping continues to rely on static, lithology-based maps with limited resolution, often lacking integration of anthropogenic and dynamic environmental factors (Rosdi et al., 2017; Banks et al., 2020). This gap is not unique to Malaysia. Globally, sinkhole monitoring systems often lag behind other hazard domains in terms of technological maturity, spatial data integration, and platform openness. Most assessments, particularly in urban settings fail to account for subsurface complexity, time-varying stressors, and human-induced triggers, leading to generalised and potentially outdated representations of risk (Banks et al., 2020; Zhang et al., 2024).

Conventional GIS-based workflows further constrain the updateability and scalability of susceptibility mapping. Manual Multi-Criteria Decision-Making (MCDM) methods, though widely used in Malaysia and elsewhere, are time-consuming, dependent on expert judgement, and unsuitable for frequent data refresh cycles. Many existing models, especially in local studies, continue to prioritise surface geology while underrepresenting critical urban factors such as underground utilities, road construction, and load-induced stress, despite growing evidence of their influence on sinkhole development (Al-Kouri et al., 2013; Bakhshipour et al., 2013; Rosdi et al., 2017; Banks et al., 2020).

In response to these limitations, this study presents a cloud-native platform for sinkhole susceptibility mapping tailored to urbanised karst environments, using Kuala Lumpur as a case study. The platform integrates fourteen geospatial control factors, spanning geological, topographic, hydrological, and anthropogenic dimensions within Google Earth Engine (GEE) for spatial processing. A lightweight one-dimensional Convolutional Neural Network (1D CNN) is implemented in Google Colab to classify pixel-based susceptibility from structured input features. This model architecture was selected for its low computational overhead and robustness with limited labelled data, making it suitable for initial deployment and future scaling. Unlike binary classifiers, the 1D CNN produces a continuous susceptibility surface, enabling more nuanced interpretation of risk gradients. The final output is deployed via a public GEE App, offering a user-friendly, updatable, and scalable platform for hazard awareness, urban planning, and early mitigation support.

While prior research by the authors (under review) benchmarked multiple models for sinkhole susceptibility in Kuala Lumpur, this paper emphasises the development and implementation of a reproducible, fully cloud-native geospatial platform. The goal is to demonstrate a scalable, publicly accessible workflow from data acquisition to web deployment, rather than algorithm comparison.

Literature Review

In Malaysia, early karst and sinkhole investigations were largely site-specific, relying on borehole data, engineering logs, and resistivity surveys to understand subsurface conditions in areas like Kuala Lumpur and Ipoh (Tan & Komoo, 1990; Zabidi & De Freitas, 2006; Bakhshipour et al., 2013). While these provided critical local insights, they lacked broader predictive value. More recent studies have adopted GIS-based methods, notably Analytic Hierarchy Process (AHP) and spatial multi-criteria evaluation, to map susceptibility based on lithology, topography, and land use (Al-Kouri et al., 2013; Rosdi et al., 2017; Banks et

al., 2020). However, these methods are static and subjective, relying on expert-assigned weights that frequently prioritise lithology at the expense of other key factors.

Nonetheless, existing approaches remain fragmented, lacking centralised public sinkhole inventory, exhibiting limited use of machine learning or dynamic data sources, and insufficiently incorporating subsurface complexity and anthropogenic influences. Although geophysical surveys and 3D models have improved site characterisation (Ahmad Nizar et al., 2022; Sulaiman et al., 2024), these are rarely incorporated into scalable mapping frameworks. As a result, existing susceptibility maps are typically static, lithology-focused, and lack real-time applicability for risk communication or planning (Banks et al., 2020).

Globally, sinkhole hazard mapping has evolved from manual aerial interpretation to automated remote sensing and machine learning approaches. Digital elevation models (e.g., SRTM, ASTER, LiDAR) and InSAR have supported topographic analysis and temporal monitoring, while GIS has enabled inventory creation and spatial correlation (Florea et al., 2002; Al-Fares, 2005; Castañeda et al., 2009; Siart et al., 2009; Weishampel et al., 2011; De Carvalho et al., 2014; Doctor & Young, 2013; Orhan et al., 2020; Garas et al., 2020; Jiang et al., 2024). Recent work integrates machine learning algorithms such as Random Forest, Support Vector Machines, Maximum Entropy, and Artificial Neural Networks for multivariate susceptibility modelling (Zhou et al., 2016; Arabameri et al., 2020; Kim et al., 2022; Bianchini et al., 2022; Abdi et al., 2024; García-Cruzado et al., 2025).

Deep learning, particularly CNNs and U-Net architectures, has enhanced spatial precision and automated detection capabilities (Alrabayah et al., 2024; Park et al., 2024; Yavariabdi et al., 2023). Yet despite algorithmic advances, few studies have translated these models into operational, user-oriented platforms. Public-facing tools such as FEMA's National Risk Index in the United States and NADMA's disaster portal in Malaysia have demonstrated the utility of interactive, map-based platforms for communicating flood, landslide, and other geohazard risks. However, comparable systems for sinkhole hazards are notably lacking, especially in urbanised karst settings. For other hazards, cloud-native implementations have begun to gain traction, for example, Varnier (2024) proposed an open-source cloud-based landslide susceptibility mapping framework using collaborative and updatable geospatial layers.

Although 1D CNNs have not been widely applied in sinkhole susceptibility mapping to date, they have shown strong performance in related tasks such as landslide and flood susceptibility assessment, as well as debris flow prediction (Ullah et al., 2022; Huang et al., 2024; Wei et al., 2024). These applications demonstrate the potential of 1D CNNs to handle

structured environmental data efficiently, supporting their use in scalable, cloud-based geohazard mapping frameworks such as the one proposed in this study. Unlike 2D CNNs, 1D CNNs operate directly on feature vectors without requiring data reshaping, reducing computational overhead and simplifying implementation (Singh et al., 2021; Ye et al., 2023). Their relatively shallow architecture, with fewer trainable parameters, lowers the risk of overfitting, an advantage for pilot testing or areas with limited training data. Recent evaluations also suggest that 1D CNNs can outperform 2D CNNs when applied to one-dimensional structured or sequential data, owing to their lower complexity, faster training time, and compatibility with real-time or cloud-based workflows (Huang et al., 2024). Despite their simplicity, 1D CNNs remain capable of capturing essential spatial feature relationships relevant to sinkhole susceptibility prediction (Singh et al., 2021).

Methodology

This study builds upon a previous investigation (currently under review) that evaluated various modelling techniques for sinkhole susceptibility in Kuala Lumpur. From that work, a 1D CNN model was selected for this paper due to its superior performance and computational efficiency. The following sections describe a fully cloud-native workflow for sinkhole susceptibility mapping, integrating multi-source spatial data, deep learning, and public web deployment using open-source platforms. The end-to-end pipeline was implemented through GEE for data preprocessing, Google Colab for model training, and the GEE App interface for interactive dissemination.

As shown in Figure 1, the workflow begins with spatial data processing in GEE, followed by training a 1D CNN in Google Colab, and ends with deployment of the output via an interactive GEE-based web application. The entire pipeline runs on cloud services, removes the need for desktop GIS software and enables reproducibility, accessibility, and future expansion.

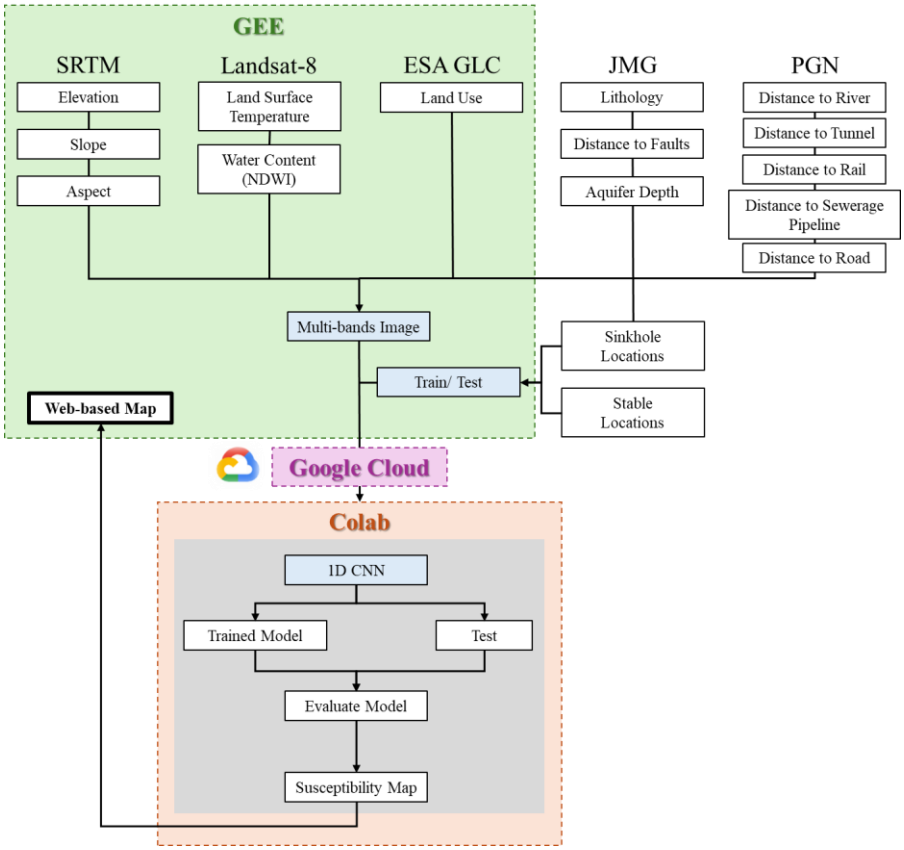

Figure 1: Overview of the Cloud-Native Workflow for Sinkhole Susceptibility Mapping using GEE, Google Colab, and GEE App Deployment.

a. Study Area Context:

The study area covers the full administrative boundary of Kuala Lumpur and selected adjacent areas in Selangor to capture regional lithological transitions and external urban influences. This region sits atop the Silurian-age Kuala Lumpur Limestone Formation (Gobbett, 1964; Hutchison & Tan, 2009), a karstified carbonate bedrock known for subsurface instability. The formation is prone to dissolution processes driven by tropical rainfall and groundwater circulation, resulting in the development of subsurface cavities, sinkholes, and irregular bedrock topography. These features are often masked by variable overburden materials, including man-made fill, alluvial deposits, and residual mining spoil from historic tin extraction (Tan, 2006; Hutchison & Tan, 2009), making subsurface interpretation particularly challenging.

The overlying land use comprises extensive infrastructure such as roads, tunnels, railways, and high-rise buildings, making Kuala Lumpur a critical hotspot for sinkhole formation due to anthropogenic loading, water leakage, and groundwater drawdown. Given this complex interplay between geology and urbanisation, Kuala Lumpur presents an ideal testbed for cloud-native geospatial hazard mapping.

Figure 2 shows the study area boundary highlighting known karst zones based on geological maps. It should be noted that these maps reflect only surface lithology, the actual subsurface extent of karst formations is uncertain and may differ due to overburden, structural complexity, and data limitations.

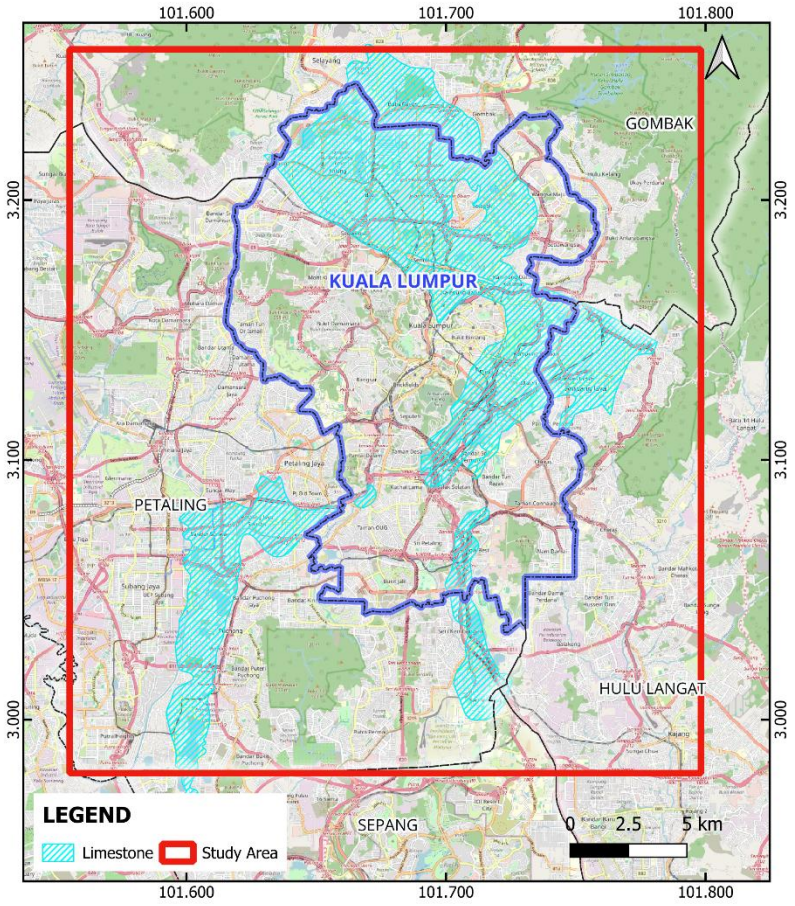

Source: Department of Mineral and Geoscience Malaysia (JMG)

Figure 2: Study Area Location (red) with Major Karst Terrain indicated (dashed blue).

b. Geospatial Data Acquisition and Processing in GEE:

Fourteen control factors influencing sinkhole formation were identified based on a combination of established sinkhole susceptibility literature and data availability. These include topographic, geological, hydrological, and anthropogenic factors (Table 1). While additional variables may be used in other studies, such data were unavailable or inaccessible for the present research and thus excluded. All datasets were accessed and processed within GEE, resampled to 30 m resolution, and combined into a single multi-band raster composite, which served as the input dataset for model training.

Table 1: Summary of Input Datasets and Derived Control Factors.

Category	Control Factor	Data Source	Platform/ Provider
Topographic	Elevation, Slope, Aspect	SRTM	GEE
Geological	Lithology, Fault Distance	Geological map, Fault lines	JMG
Hydrological	Groundwater Depth	Well data	JMG
	NDWI (Normalised Difference Water Index)	Landsat-8 imagery	GEE
	Distance to Rivers	River layer	PGN
Anthropogenic	LST (Land Surface Temperature)	Landsat-8 imagery	GEE
	Land Use	ESA Urban Atlas	GEE
	Distance to Roads, Railways, Tunnels, Pipelines	Infrastructure maps	PGN

(GEE = Google Earth Engine; JMG = Department of Mineral and Geoscience Malaysia; PGN = National Geospatial Centre Malaysia; ESA = European Space Agency)

c. Sample Labelling and Export to Google Colab:

High-susceptibility samples were generated by applying 30 m buffer around known sinkhole locations obtained from the Department of Mineral and Geoscience Malaysia (JMG) through a formal request in 2024. These buffered zones represent reported areas of ground deformation. In contrast, low-susceptibility samples were manually selected from geologically stable zones with minimal influence from known conditioning factors. A total of 68 labelled points (34 high-susceptibility and 34 low-susceptibility) were used. These labelled samples (1 = high, 0 = low) were rasterised and exported from GEE as a structured CSV (Comma-Separated Values) file, a widely used text format for storing structured tabular data. The samples along with the composite image were uploaded to Google Cloud Storage and accessed in Colab for model training.

d. Model Training in Colab (1D CNN):

A 1D CNN was implemented using Keras in Google Colab to classify sinkhole susceptibility based on the 14 input features. This architecture is well suited to structured, tabular input and offers efficient performance with minimal training data. The model architecture included two sequential convolutional layers (with 32 and 64 filters respectively), each followed by a Rectified Linear Unit (ReLU) activation, max pooling, and dropout regularisation layers. ReLU functions introduce non-linearity by zeroing out negative values, enabling the model to capture complex feature interactions. Max pooling reduces the spatial resolution of feature maps while retaining the most relevant activations, and dropout helps reduce overfitting by randomly deactivating neurons during training. The

final dense output layer used softmax activation to produce a probability distribution across the two classes: low (0) and high (1) susceptibility zones.

The input data were reshaped into a three-dimensional tensor of shape [samples, features, 1] to match the expected input of the Keras 1D CNN model. Class labels were one-hot encoded to support softmax-based categorical classification. The model compilation was performed using the Adam optimiser and trained up to 100 epochs with early stopping based on validation loss to prevent overfitting, using a batch size of 8 and an 80/20 stratified train-test split across the 68 labelled samples (34 high-risk and 34 low-risk zones).

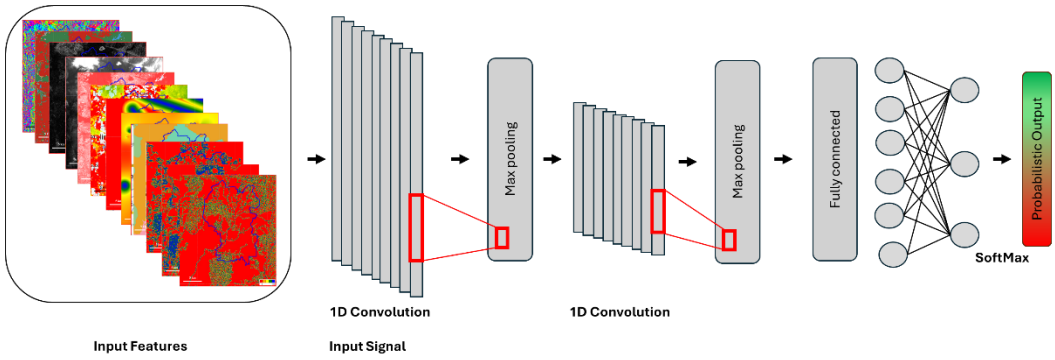

Figure 3: Architecture of the 1D CNN Model Implemented in Google Colab.

e. Susceptibility Prediction and Export to GEE:

After training, the model was applied to the entire study area using a pixel-wise inference on the multi-band raster. The model generated a continuous susceptibility map with values ranging from 0 (low risk) to 1 (high risk). This probabilistic surface allows smoother transitions between susceptibility classes, improving visual interpretability compared to binary outputs.

To assess performance, the Area Under the Receiver Operating Characteristic Curve (AUC-ROC) was used as the validation metric, which offers a threshold-independent measure of the model's class separability and prediction robustness.

The prediction output was exported back to Google Cloud Storage as a GeoTIFF, a standard raster image format used for geospatial data that retains coordinate information, allowing integration into the GEE platform for public-facing visualisation.

f. Deployment as Interactive Web Application in GEE:

The GeoTIFF output was re-imported into GEE, where it was visualised alongside base layers such as terrain and infrastructure. The interface elements were configured to include a colour-coded legend, clickable features, and tooltips to support user interaction. Metadata fields such as data source, model type, and control factor source were embedded where

supported. Finally, the interactive map was published via the GEE App interface by enabling public access and generating a shareable URL. The web interface was designed with flexibility in mind, enabling the integration of additional visual layers or tools as required. The cloud-native setup supports low maintenance, straightforward updates, and easy adaptation to other cities or geohazards.

Results and Discussion

a. Cloud Deployment Outcome:

The final susceptibility map was deployed using the GEE App platform. The interface includes: (1) Toggleable layers (susceptibility and topography), (2) An interactive click function displays the district/ subdistrict and the number of recorded sinkhole events, and (3) Colour-coded points (red = sinkhole present, green = none) for intuitive interpretation.

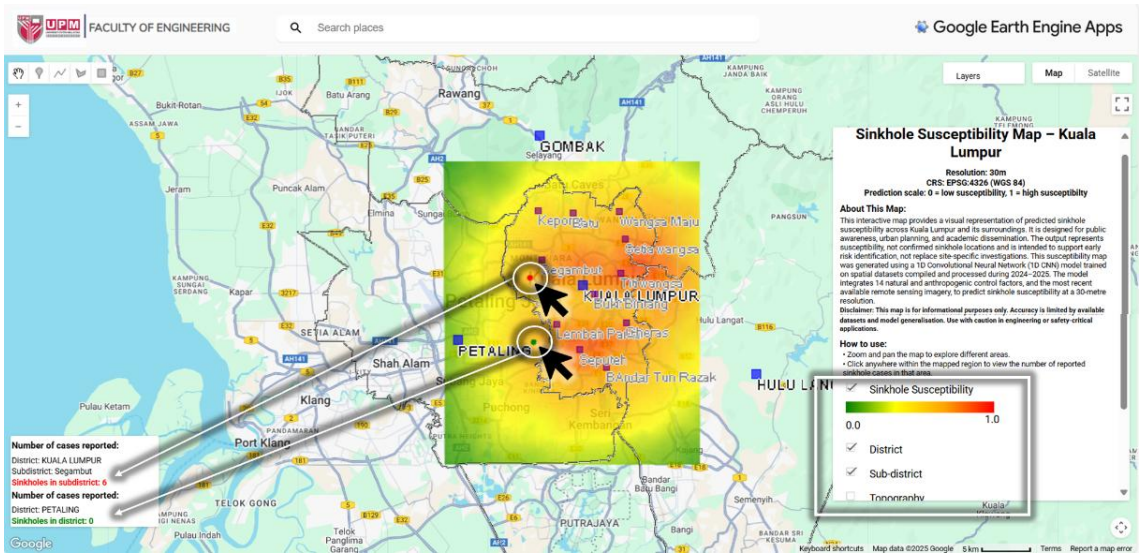

Figure 4: Public-Facing GEE Web Application Showing the Sinkhole Susceptibility Layer with Interactive Features.

The final deployment demonstrates the feasibility of integrating open cloud platforms to automate the full geospatial modelling lifecycle from raw data to actionable, interactive output. The modular nature of the pipeline supports future upgrades such as: (1) Incorporation of real-time or time-series inputs (e.g., InSAR), (2) Expansion to other urban karst regions, and (3) Integration with urban planning systems.

This system eliminates the need for proprietary desktop tools, enabling scalable deployment and broader stakeholder accessibility.

b. Susceptibility Map Output:

The final product of the pipeline is a continuous susceptibility surface with values ranging from 0 (low risk) to 1 (high risk). High-risk zones correspond primarily to areas with intense

urban development atop the Kuala Lumpur Limestone Formation, including zones with dense infrastructure and historical sinkhole records. This output supports nuanced interpretation of risk zones and aligns with the goal of communicating gradual susceptibility transitions rather than binary thresholds.

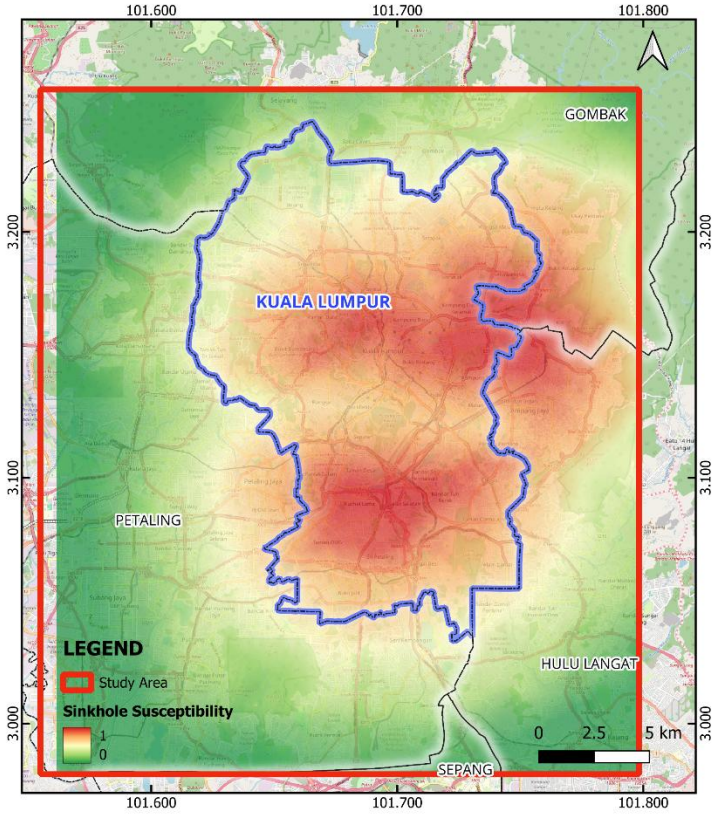

Figure 5: Final Sinkhole Susceptibility Output Generated by the Cloud-Native Pipeline.

c. Model Performance:

Although model performance was not the primary focus, validation was conducted using a stratified 80/20 split. The 1D CNN achieved a high AUC–ROC (0.97), indicating strong separability between classes. This confirms that even a lightweight model can produce reliable susceptibility predictions, highlighting the model's reliability for use within a cloud-native, publicly accessible risk communication platform.

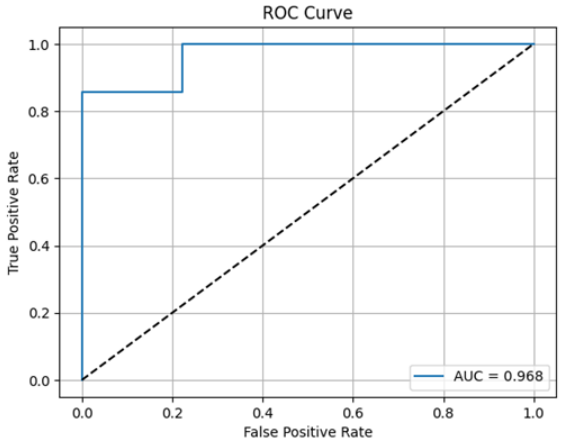

Figure 6: Receiver Operating Characteristic (ROC) Curve for 1D CNN Model.

d. Practical Implications and Limitations:

This study demonstrates the real-world applicability of a scalable, cloud-native geospatial pipeline for sinkhole susceptibility mapping. This pipeline produced reliable, continuous susceptibility predictions using a minimal training set, demonstrating its suitability for early-stage or prototype deployments, particularly in settings where sinkhole inventory data remain sparse, inconsistent, or incomplete. Key strengths include: (1) End-to-end automation of data preparation, training, and deployment, (2) Open access via an intuitive web application, and (3) Flexibility to integrate updated datasets or new study areas.

Deployment via a GEE-based interactive application provides a scalable, low-maintenance solution for local governments and infrastructure agencies, where the tool supports dynamic risk communication and can inform proactive urban planning or mitigation strategies. However, several limitations remain: (1) The sinkhole inventory is limited in size, spatial coverage, and lacks attributes such as trigger type or severity; (2) The model relies mainly on surface and infrastructure-level factors but does not sufficiently incorporate subsurface data (e.g., karst complexity) and groundwater fluctuations; (3) Static environmental features only, temporal dynamics (e.g., changes in land use or infrastructure) not yet included.

Future enhancements should consider: (1) Integration of subsurface geophysical data and groundwater sensor data; (2) Use of time-series remote sensing inputs (e.g., InSAR deformation analysis); (3) Expanding the inventory through crowdsourcing or public reporting; (4) Scaling the platform for use in other karst-prone cities for comparative studies or regional-scale modelling; (5) Testing more advanced architectures such as U-Net or transformer-based models. Despite these limitations, the current platform provides a foundational framework for dynamic, scalable sinkhole susceptibility assessment and represents a step forward in hazard mapping for rapidly urbanising karst landscapes.

Conclusion and Recommendation

A fully cloud-native platform for sinkhole susceptibility mapping was successfully developed using Google Earth Engine and Google Colab. This end-to-end workflow integrates multi-source spatial data, a lightweight deep learning model, and an interactive web application to deliver interpretable and accessible risk information.

The 1D CNN model produced a continuous susceptibility surface with strong AUC–ROC performance (0.97), demonstrating robust predictive capability despite limited training data. The resulting pipeline offers a replicable, low-resource geospatial solution for other urbanised karst regions, providing practical benefits for planners, engineers, and the public, without reliance on desktop GIS or specialised software.

This work addresses key gaps in current sinkhole risk communication approaches by delivering a reproducible, fully cloud-native solution for data-scarce urban environments. It serves as a prototype for future expansion at regional or national deployment and showcases the feasibility of combining cloud-based geospatial tools with machine learning in operational hazard mapping.

Future developement should focus on incorporating dynamic or temporal datasets, such as InSAR-based deformation monitoring, real-time groundwater sensors, and updated infrastructure layers to improve temporal sensitivity. Strengthening sinkhole inventory systems through community-sourced reporting and expanding access to subsurface data will further enhance model robustness and practical deployment potential.

This study differs from previous model-centric research by demonstrating the feasibility of an end-to-end, cloud-native deployment pipeline. Rather than focusing solely on algorithmic performance, the emphasis here lies in delivering a scalable, reproducible, and publicly accessible geospatial solution for sinkhole susceptibility mapping in rapidly urbanising karst landscapes.

Acknowledgement

The author gratefully acknowledges the Department of Minerals and Geoscience Malaysia (JMG) and the National Geospatial Centre (PGN) for providing key geospatial datasets used in this study. The computational workflow was supported by open-access platforms including Google Earth Engine, Google Colab, and Google Cloud Console. Special thanks are extended to Sr Gs Dr Siti Nur Aliaa Roslan for academic guidance throughout the research.

References

Abdi, B., Kolo, K., & Shahabi, H. (2024). Assessment of Land Degradation Susceptibility within the Shaqlawa Subregion of Northern Iraq-Kurdistan Region via Synergistic Application of Remotely Acquired Datasets and Advanced Predictive Models. Environ Monit Assess, Vol. 196(1103). https://doi.org/10.1007/s10661-024-13284-9

Ahmad Nizar, N.H., Khong, L.X., Ismail, S., Ahmad, F., & Zabidi, H. (2022). Characterization of Kuala Lumpur Bedrock Subsurface Limestone Aquifer System by using Borehole Modelling Analysis. Materials Today: Proceedings, Vol. 66(5). https://doi.org/10.1016/j.matpr.2022.07.333

Al-Fares, R. A. (2005). The Utility of Synthetic Aperture Radar (SAR) interferometry inmonitoring sinkhole subsidence: subsidence of the Devil's Throat Sinkhole Area (Nevada, USA). Sinkholes and the Engineering and Environmental Impactsof Karst. https://doi.org/10.1061/40796(177)57

Al-Kouri, O., Al-Fugara, A., Al-Rawashdeh, S., Sadoun, B., & Pradhan, B. (2013). Geospatial Modeling for Sinkholes Hazard Map Based on GIS & RS Data. Journal of Geographic Information System, Vol. 5(6). https://doi.org/10.4236/jgis.2013.56055

Alrabayah, O., Caus, D., Watson, R.A., Schulten, H.Z., Weigel, T., Rüpke, L., & Al-Halbouni, D. (2024). Deep-Learning-Based Automatic Sinkhole Recognition: Application to the Eastern Dead Sea. Remote Sens., Vol. 16(13). https://doi.org/10.3390/rs16132264

Arabameri, A., Saha, S., Roy, J., Tiefenbacher, J.P., Cerda, A., Biggs, T., Pradhan, B., Thi Ngo, P.T., & Collins, A.L. (2020). A Novel Ensemble Computational Intelligence Approach for the Spatial Prediction of Land Subsidence Susceptibility. Sci Total Environ., Vol. 726. https://doi.org/10.1016/j.scitotenv.2020.138595

Bakhshipour, Z., Huat, B.B.K., Ibrahim, S., Asadi, A., & Kura, N.U. (2013). Application of Geophysical Techniques for 3D Geohazard Mapping to Delineate Cavities and Potential Sinkholes in the Northern Part of Kuala Lumpur, Malaysia. The Scientific World Journal, Vol. 1. https://doi.org/10.1155/2013/629476

Banks, V., Affandi, E., Ng, T.F., Arnhardt, C., Ramli, Z., Ahmad, F., Pereira, J., & Reeves, H., (2020). Sinkhole Susceptibility Mapping in the Kuala Lumpur and the Need for a Buried Karst Database. *Proceedings Of The 16th Multidisciplinary Conference on Sinkholes and The Engineering and Environmental Impacts of Karst.*

Bianchini, S., Confuorto, P., Intrieri, E., Sbarra, P., Di Martire, D., Calcaterra, D., & Fanti, R. (2022). Machine Learning for Sinkhole Risk Mapping in Guidonia-Bagni di Tivoli Plain (Rome), Italy. Geocarto International, Volume 37(27). https://doi.org/10.1080/10106049.2022.2113455

Castañeda, C., Gutiérrez, F., Manunta, M., & Galve, J. (2009). DInSAR Measurements of Ground Deformation by Sinkholes, Mining Subsidence, and Landslides, Ebro River, Spain. Earth Surf. Process. Landforms, Vol. 34(11). https://doi.org/10.1002/esp.1848

Damayanti, A., Riadini, F., & Pamungkas, F.D. (2021). Potential Areas of Land Subsidence in Karst Landscape: Case Study in Ponjong and Semanu District, Gunungkidul Regency, Yogyakarta, Indonesia. International Journal on Advanced Science Engineering Information Technology, Vol. 11(2). https://doi.org/10.18517/ijaseit.11.2.6754

De Carvalho, O. A., Júnior, Guimarães, R. F., Montgomery, D. R., Gillespie, A. R., Trancoso Gomes, R. A., De Souza Martins, É., & Silva, N. C. (2014). Karst Depression Detection Using ASTER, ALOS/PRISM and SRTM-Derived Digital Elevation Models in the Bambuí Group, Brazil. Remote Sens., Vol. 6(1). https://doi.org/10.3390/rs6010330

Doctor, D.H., & Young, J.A., (2013). An Evaluation of Automated GIS Tools for Delineating Karst Sinkholes and Closed Depressions from 1-Meter LiDAR-Derived Digital Elevation Data. *13th Multidisciplinary Conference on Sinkholes and the Engineering and Environmental Impacts of Karst.*

Fartihul Ilmy, H, Darminto, M.R. & Widodo,A., (2021). Application of Machine Learning on Google Earth Engine to Produce Landslide Susceptibility Mapping (Case Study: Pacitan). *IOP Conf. Series: Earth and Environmental Science.*

Florea, L.J., Paylor, R.L., Simpson, L., and Gulley, J., (2002). Karst GIS advances in Kentucky. *J. CaveKarst St., Volume 64(1).*

Ford, D.C. & Williams, P.W. (2007). Karst Hydrogeology and Geomorphology. Wiley.

Garas, K.L., Madrigal, M.F.B., Agot, R.D.D., Canlas, M.C.M., & Manzano, L.S.J. (2020). Karst Depression Detection using IFSAR-DEM：A Tool for Subsidence Hazard Assessment in Panglao, Bohol [J]. Carsologica Sinica, Vol.39(6). https://doi.org/10.11932/karst20200612

García-Cruzado, S.A., Ramírez-Serrato, N.L., Herrera-Zamarr´on, G.S., Hernandez-Hernandez, M.A., Y´epez-Rinc´on, F.D., Villarreal, S., & Olea-Olea, S. (2025). Mapping Sinkhole Susceptibility in Mexico City Using the Weight of Evidence Method. Journal of South American Earth Sciences, Vol. 153. https://doi.org/10.1016/j.jsames.2025.105368

Gobbett, D.J. (1964). The Lower Paleozoic Rocks of Kuala Lumpur, Malaysia. *Federation Museums Jour., Volume 9 (New Series).*

Gutiérrez, F., Parise, M., De Waele, J., & Jourde, H. (2014). A Review on Natural and Human-induced Geohazards and Impacts in Karst. Earth-Science Reviews, Vol. 138. https://doi.org/10.1016/j.earscirev.2014.08.002

Ha, K.M. (2024). Coping with Sinkholes: A Systematic Literature Review. Journal of Environmental & Earth Sciences, Vol. 6(3). https://doi.org/10.30564/jees.v6i3.6812

Huang, H., Wang, Z., Liao, Y., Gao, W., Lai, C., Wu, X., and Zeng, Z. (2024). Improving the explainability of CNN-LSTM-based flood prediction with integrating SHAP technique. Ecological Informatics, Vol. 84. https://doi.org/10.1016/j.ecoinf.2024.102904

Hutchison, C.S. & Tan, D.K. (2009). Geology of Peninsular Malaysia. University of Malaya and the Geological Society of Malaysia.

Jia, L., Meng, Y., Li, L., & Yin, R. (2021). A Multidisciplinary Approach in Cover-collapse Sinkhole Analyses in the Mantle Karst from Guangzhou City (SE China). Nat Hazards, Vol. 108. https://doi.org/10.1007/s11069-021-04738-1

Jiang, Z., Hu, S., Deng, H., Wang, N., Zhang, F., Wang, L., Wu, S., Wang, X., Gao, Z., Chen, Y., & Li, S. (2024). Detection and Automatic Identification of Loess Sinkholes from the Perspective of LiDAR Point Clouds and Deep Learning Algorithm. Geomorphology, Vol. 465. https://doi.org/10.1016/j.geomorph.2024.109404

Kim, Y.J., Nam, B.H., Jung, Y., Liu, X., Choi, S., Kim, D., & Kim, S. (2022). Probabilistic Spatial Susceptibility Modeling of Carbonate Karst Sinkhole. Engineering Geology, Vol. 306. https://doi.org/10.1016/j.enggeo.2022.106728

Li, P., Bai, M, Wei, Z, Li,X., & Shi, H. (2022). Stability Analysis of Subgrade under Dynamic Loading of Single and Double High-Speed Railways in Karst Areas. KSCE J Civ Eng, Vol. 26(8). https://doi.org/10.1007/s12205-022-1308-6

Li, B., Wang, H., & Tang H. (2024). Investigating the Drivers of Urban Cover-Collapse Sinkholes in Shanghai: Analyzing Dominant Factors and Proposing Mitigation Strategies. Anthropocene Coasts, Vol. 7(18). https://doi.org/10.1007/s44218-024-00051-z

Mohammadi-Ahmadmahmoudi, P., Khaleghi, S., & Ehteshami-Moinabadi, M. (2025). Doline Susceptibility Mapping Using Multisource Data in the Karst Aquifers of Saldaran Mountain, High Zagros Belt. Journal of Mountain Science, Vol. 22. https://doi.org/10.1007/s11629-024-8834-2

Orhan, O., Yakar, M., & Ekercin, S. (2020). An Application on Sinkhole Susceptibility Mapping by Integrating Remote Sensing and Geographic Information Systems. Arabian Journal of Geoscience, Vol. 13(886). https://doi.org/10.1007/s12517-020-05841-6

Park, J.H., Kang, J., Kang, J., & Mun, D. (2022). Machine-learning-based Ground Sink Susceptibility Evaluation Using Underground Pipeline Data in Korean Urban Area. Sci Rep, Vol. 12(1). https://doi.org/10.1038/s41598-022-25237-8

Park, J.H., Kim, J., Lee, S., Kang, J., & Mun, D. (2024). Hybrid MLP-CNN-based Ground Sink Susceptibility Prediction in Urban Area Using Underground Pipe Map. Reliability Engineering and System Safety, Vol. 245. https://doi.org/10.1016/j.ress.2024.110031

Rosdi, M.A.H.M., Othman, A.N., Zubir, M.A.M., Latif, Z.A., & Yusoff, Z.M. (2017). Sinkhole Susceptibility Hazard Zones Using GIS and Analytical Hierarchical Process (AHP): A Case Study of Kuala Lumpur and Ampang Jaya. *The International Archives of the Photogrammetry, Remote Sensing and Spatial Information Sciences XLII-4/W5.*

Shi, X., Zhang, S., Jiang, M., Pei, Y., Qu, T., Xu, J., & Yang C., (2021). Spatial and Temporal Subsidence Characteristics in Wuhan (China), during 2015-2019, Infrared from Sentinel-1 Synthetic Aperture Radar (SAR) Interferometry. Nat. Hazards Earth Syst. Sci., Vol. 21. https://doi.org/10.5194/nhess-21-2285-2021

Siart, C., Bubenzer, O., & Eitel, B. (2009). Combining Digital Elevation Data (SRTM/ASTER), High Resolution Satellite Imagery (Quickbird) and GIS for Geomorphological Mapping: A Multi-component Case Study on Mediterranean Karst in Central Crete. Geomorphology, Vol. 112. https://doi.org/10.1016/j.geomorph.2009.05.010

Singh, K., Mahajan, A., & Mansotra, V. (2021). 1D-CNN based Model for Classification and Analysis of Network Attacks. International Journal of Advanced Computer Science and Applications, Vol. 12(11). http://dx.doi.org/10.14569/IJACSA.2021.0121169

Sulaiman, M.S.S., Hussin, H., & Abiyoga, M., (2024). Sinkhole Investigation using Resistivity Method in Universiti Malaysia Kelantan, Jeli Campus. *BIO Web Conf.*

Tan, B.K. & Komoo, I. (1990). Urban Geology: Case Study of Kuala Lumpur, Malaysia. Engineering Geology, Vol. 28. https://doi.org/10.1016/0013-7952(90)90034-X

Tan, B.K., (2006). Urban Geology of Kuala Lumpur and Ipoh, Malaysia. *IAEG, Volume 24.*

Ullah, K., Wang, Y., Fang, Z., Wang, L., and Rahman, M. (2022). Multi-hazard susceptibility mapping based on Convolutional Neural Networks. Geoscience Frontiers, Vol. 13(5). https://doi.org/10.1016/j.gsf.2022.101425

Varnier, M. (2024). A Cloud-based and Open-source Approach to Generate Landslide Susceptibility Map. Revista Brasileira de Geomorfologia, Vol. 25(2). https://doi.org/10.20502/rbgeomorfologia.v25i2.2491

Waltham, T., Bell, F., & Culshaw, M., (2005). Sinkholes and Subsidence: Karst and Cavernous Rocks in Engineering and Construction. Springer.

Weishampel, J.F., Hightower, J.N., Chase, A.F., Chase, D.Z., & Patrick, R.A. (2011). Detection and Morphologic Analysis of Potential Below-canopy Cave Openings in the Karst Landscape around the Maya Polity of Caracol Using Airborne LiDAR. Journal of Cave and Karst Studies, Vol. 73(3). https://doi.org/10.4311/2010EX0179R1

Wei, X., Gardoni, P., Zhang, L., Tan, L., Liu, D., Du, C., and Li, H. (2024). Improving pixel-based regional landslide susceptibility mapping. Geoscience Frontiers, Vol. 15(4). https://doi.org/10.1016/j.gsf.2024.101782

Yavariabdi, A., Kusetogullari, H., Orhan,O., Uray, E., Demir, V., Celik, T., & Mendi, E. (2023). SinkholeNet: A Novel RGB-slope Sinkhole Dataset and Deep Weakly-supervised Learning Framework for Sinkhole Classification and Localisation. The Egyptian Journal of Remote Sensing and Space Science, Vol. 26. https://doi.org/10.1016/j.ejrs.2023.10.006

Ye, X., Cao, Y., Liu, A., Wang, X., Zhao, Y., & Hu, N. (2023). Parallel Convolutional Neural Network toward High Efficiency and Robust Structural Damage Identification. Structural Health Monitoring, Vol. 22(6). https://doi.org/10.1177/14759217231158786

Yumba, j., Ferentinou, M., & Grobler, M. (2024). Experimental Study of sinkhole Propagation Induced by a Leaking Pipe Using Fibre Bragg Grating Sensors. Sensors, Vol. 24(19). https://doi.org/10.3390/s24196215

Zabidi, H. & De Freitas, M.H., (2006). Structural Studies for the Prediction of Karst in the Kuala Lumpur Limestone. *IAEG The Geological Society of London, Volume 264.*

Zhang, Y., Jiao, Y., He, L., Tan, F., Zhu, H., Wei, H., & Zhang, Q. (2024). Susceptibility Mapping and Risk Assessment of Urban Sinkholes based on Grey System Theory. Tunnelling and Underground Space Technology incorporating Trenchless Technology Research, Vol. 152. https://doi.org/10.1016/j.tust.2024.105893

Zhou, G., Yan, H., Chen, K., & Zhang, R. (2016). Spatial Analysis for Susceptibility of Second-time Karst Sinkhole: A Case Study of Jili Village in Guangxi, China. Computer & Geosciences, Vol. 89. https://doi.org/10.1016/j.cageo.2016.02.001